Determining CO2 Balance influenced by Upwelling and Primary Production in the Equatorial Pacific Region at 180° using CO2 and O2 flux

Amrita Ahuja

06/02/23

University of Washington

School of Oceanography, Box 357940

Seattle WA 98195-7940

amritaa@uw.edu

Abstract

The oceanic carbon cycle is one of the most important mechanisms in controlling the Earth's climate as oceans take up to 30% of the carbon emissions, acting as a major sink. The ocean's biological and solubility pumps are responsible for carbon storage through air-sea interactions. However, a big source of carbon to the atmosphere is the Equatorial Pacific due to it being a region of upwelling where old carbon-rich waters from the deep sea are transported to the surface. This paper highlights the finding of the research conducted upon the RV Thompson from 2nd to 8th March, 2023 in the Equatorial Pacific along the 5°N to 5°S transect during the tail end of a La Niña event. In order to quantify the air-sea flux and the proportion of carbon balance affected by upwelling and primary production in this region, a 1-D carbon budget model in steady state was applied to the CO_2 and O_2 distributions between 2°N and 2°S at the dateline (180°). Gas transfer velocity and solubility coefficients were used to quantify the outgassing of CO_2 and to understand the correlation strength of these factors. Using the model, 96% of the flux of CO_2 is affected by upwelling and less than 4% is affected by primary production. The average F_{CO2} = 0.0120 mol m^{-2} day^{-1} from 2°N to 2°S due to the proximity to the equator but the highest flux out of the system was 0.0227 mol m^{-2} day^{-1}, recorded at 3°N with gas transfer velocity of CO_2 ~27 cm/hr at a wind speed of 11 m/s, after which the wind speeds became relatively constant proceeding 2°N. This indicated that even though biochemical factors play a dominant role in regulating air-sea flux, physical factors such as wind are quite important as well.

Plain Language Summary

The oceans have been taking up carbon at a rapid pace over the last century and is predicted to keep doing so in order to compensate the anthropogenic emissions and regulate climate

change. The oceans are also a major source of oxygen as it contributes to almost half of the world's primary production and conversion of inorganic carbon to organic matter. However, one of the biggest sources of carbon is the equatorial Pacific, where carbon dioxide leaves the system rather than staying or being converted. To understand how the ocean interacts with the atmosphere, a simple carbon budget model is hypothesized to be calculated along the transect closest to the equator and with environmental conditions that are similar to each other (2°N to 2°S) at 180°. The model considers physical factors such as wind and salinity and also biochemical factors such as oxygen proxy for primary production and upwelling of carbon rich waters. This region was outgassing carbon, averaged out to a positive flux of 0.01204 mol m^{-2} day^{-1} while the oxygen flux was averaged to be -0.000009 mol m^{-2} day^{-1} , implying that primary production was not able to overcome the amount of inorganic carbon being upwelled to the surface. Then using the estimated model, calculations showed that upwelling contributed to 96% of the flux while primary production contributed <4%. Furthermore, on an annual scale, the carbon flux = 4.4 mol m^{-2} yr^{-1} , quite similar to previous studies conducted during muted El Niño events, with a flux out of the system. These factors together, can then help in understanding the magnitude of influence on carbon concentrations in the mixed layer and atmosphere, assuming steady state conditions, and possibly over large time scales as well if further research is conducted.

Introduction

The global ocean is an integral component of the carbon cycle acting as a mediator between climate change and the planet's response to it. Over the course of the last 30 years, anthropogenic carbon emissions have been increasing and thus increasing the concentration of atmospheric carbon dioxide (CO_2) (Hauck et al, 2020). Since the 1850s, the global ocean has taken up 26% of the atmospheric CO_2 emissions

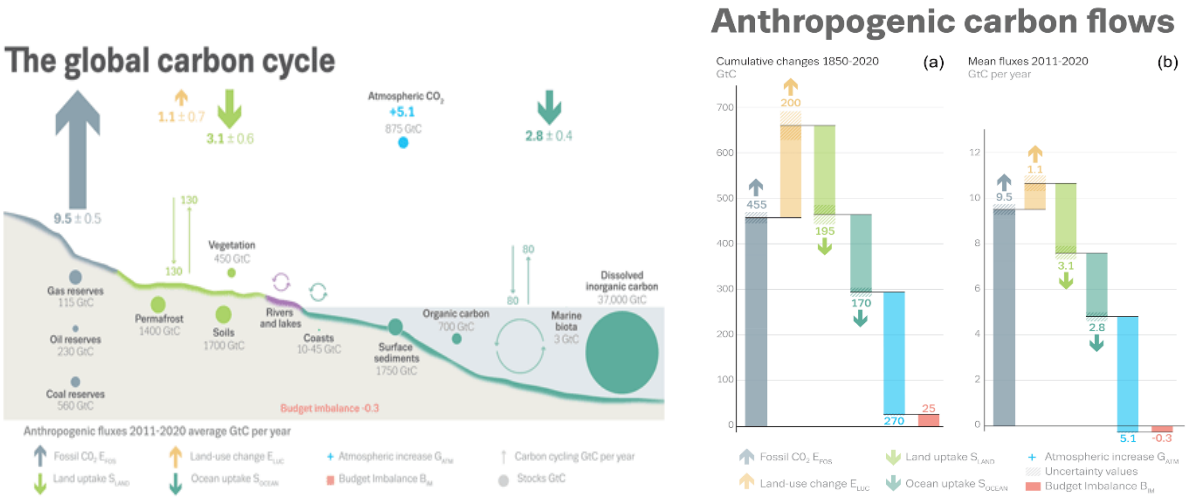

A) B)

Figure 1: Quantification of the A) carbon dioxide fluxes in the scope of the global carbon cycle from 2011-2020 and B) Mean carbon dioxide fluxes (GtC) from 2011-2020 using different sources (Friendlingstein et al, 2022)

and recently in 2020 presumably contributed as one of the major carbon sinks by uptaking 2.8 ± 0.4 GtC yr−1 in the past decade (Fig 1) (Friedlingstein et al. 2022). The CO_2 gas interaction between the ocean and atmosphere is known as the air-sea flux and helps in equilibrating the CO_2 (Gruber et al, 2009). It's one of the most predominant processes in determining the future of the carbon cycle and forecasting future CO_2 concentrations (Takahashi et al, 2009). CO_2 flux between the ocean and the atmosphere can help determine

climate-change models as well as estimation of shallow and deep-water exchange of CO_2 gas (Brady et al, 2019).

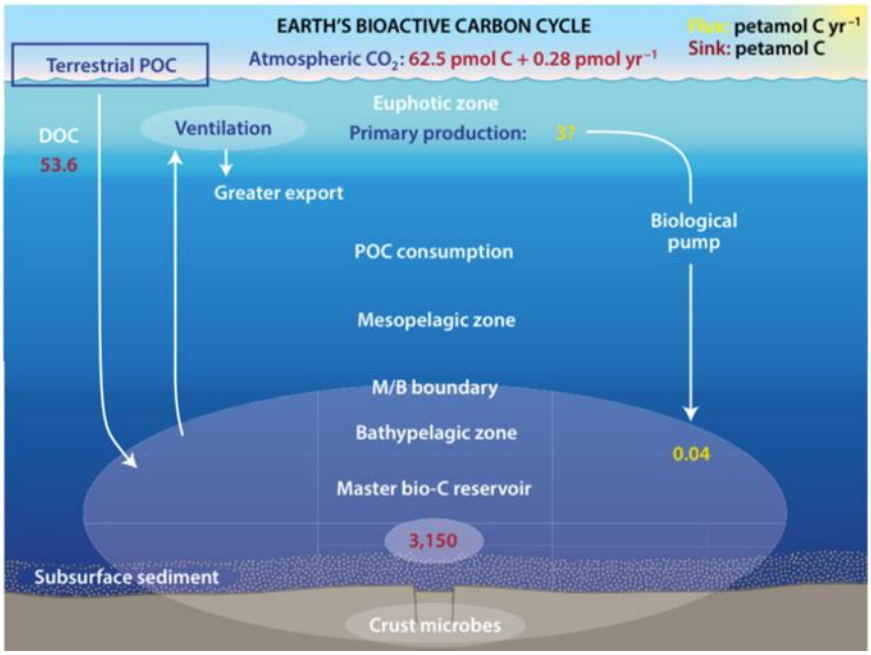

Figure 2: Diagram of the Carbon cycle and interaction of atmospheric CO_2 and biological pump (Honjo et al, 2014).

The thermodynamic equilibrium of dissolved CO_2 is maintained by the air-sea flux and can be quantified using the partial pressure of CO_2 (pCO_2) (Gloege et al,2022; Gruber et al. 2009; Sutton et al. 2017). To quantify the air-sea flux, which contributes to the global carbon cycle, measurement of partial pressure of CO_2 (pCO_2) of both the atmosphere and ocean are utilized (Gloege et al,2022 ; Gruber et al. 2009; Sutton et al. 2017). The difference in the pCO_2 of the atmosphere and the ocean

$$\Delta pCO_2 = [pCO_2]_{sw} - [pCO_2]_{atm} \quad \text{(Eq.1)}$$

helps in quantifying the magnitude of ΔpCO_2 across the surface of the water as well as identify the sources and sinks of CO_2 (Takahashi et al, 2009). In order to determine the flux (F_{CO2}) itself, gas transfer velocity (k) (Wanninkhof, 2014) and solubility coefficient (Ksol), which is dependent on sea surface temperature (SST) and sea surface salinity (SSS) (Weiss, 1974), also need to be taken into account as together they modulate the amount CO_2

absorption into the ocean (Sutton et al, 2017;Tien et al, 2019). The value of k can be fit into an empirical function of wind stress, which is why it is essential to consider wind velocity in our calculations and data observations (Wanninkhof, 2014; Tien et al, 2019). It is important to note that surface ocean pCO_2 can be perturbed by 3 main mechanisms, which then ultimately affect the overall flux: i) upwelling of cold CO_2 rich waters from deep ocean leading to outgassing of CO_2, ii) the biological pump increasing its uptake of CO_2 due to the influx of nutrients from the upwelled waters and ultimately converting dissolve inorganic carbon (DIC) to organic matter carried out by phytoplankton communities in the euphotic zone (Volk and Hoffert, 1985) (Fig.2) and the iii) solubility pump where during periods of relatively warmer surface waters the gas-exchange ability of CO_2 is lowered and leads to a flux out of the ocean while cooler surface waters increases the solubility and positively intakes CO_2 into the ocean (Friedrich et al, 2008 ; Heinze et al, 2015; Pittman et al, 2022; Volk and Hoffert,1985). Thus, air-sea flux provides an insight on the ocean's ability to act as a source or sink of CO_2 and estimate the global carbon cycle changes and impacts.

Additionally, certain anthropogenically accelerated problems such as ocean acidification and algal blooms can also be expressed using the CO_2 flux (Heinze et al, 2015).

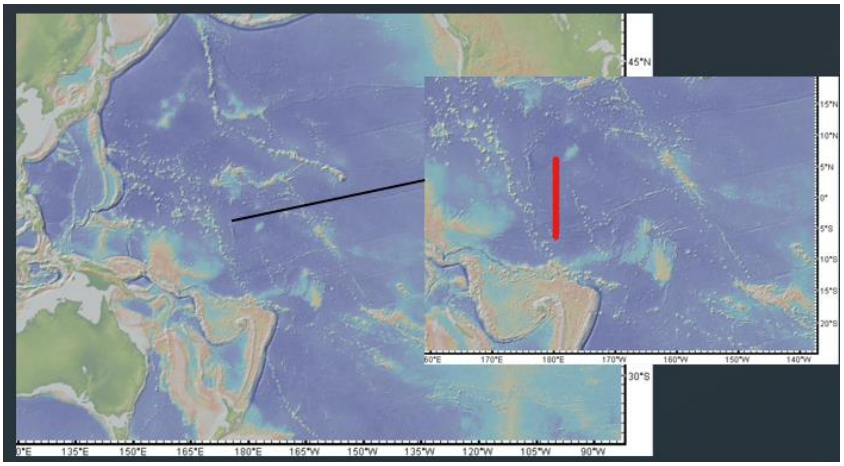

Figure 3: The red line spanning from 5N to 5S at Greenwich Meridian and has 15 data collection stations on that transect.

In contrast, rather than a sink, the Equatorial Pacific is one of the biggest open ocean sources of CO_2 releasing ~0.5GtC of CO2 yearly (Pittman et al, 2022; Takashi et al,2009; Wong et al, 2022) (https://www.pmel.noaa.gov/co2/elNiño.html). This region of the Equatorial Pacific (Fig. 3) is a region of wind-driven upwelling, which brings up cool rich DIC waters up to the surface thus increasing the pCO_2 in the surface ocean (Wong et al, 2022). Upwelling of nutrients in the equatorial Pacific drive the biological pump through high rates of primary production and uptake of CO_2 in dissolved inorganic form while also producing oxygen (O_2) (Pittman et al, 2022; Volk and Hoffert, 1985). The O_2 flux then can be used as a proxy for primary productivity in this region, especially since most of the biological activity along with both CO_2 and O_2 fluxes, tend to occur in the mixed layer depth (MLD) (Emerson and Yang, 2022). However, there is still variability in the CO_2 concentrations interannually due to the El Niño-Southern Oscillation (ENSO) (Wong et al, 2022). ENSO is hypothesized to be the largest temporal variability in CO_2 flux as it can affect the thermocline depth and trade wind speed and how long the cold period lasts (Pittman et al, 2022)(https://www.pmel.noaa.gov/co2/elNiño.html). Generally, CO_2 outgassing is muted during El Niño and extremely elevated during La Niña events, the cold phase. This phase has stronger

and richer [DIC] waters being upwelled as well as stronger trade winds, driving a more positive CO_2 flux out of the ocean (Ayar et al, 2022; Pittman et al, 2022; Tian et al, 2019; Wong et al, 2022). Currently, the ENSO cycle in the Equatorial Pacific (Fig. 3) is nearing the end of the La Niña.

Although it is difficult to estimate the CO_2 flux due to various temporal, physical and biochemical factors all working together to influence the flux, this paper aims to provide a quantification of the ΔpCO_2 and primary productivity in order to understand a simple 1D carbon budget model in the Equatorial Pacific at 180°.

Hypothesis

The equatorial Pacific at the International Dateline (180°) is a region of upwelling where CO_2 flux outgasses to the atmosphere as $pCO_{2SW} > pCO_{2Atm}$. Due to the equatorial Pacific being such a strong source of CO_2, it's important to consider that surfacing waters are older have had mostly respiration occurring due to lack of sunlight, so nutrients such as dissolved O_2 concentrations may be significantly lowered.

However, this flux out of the ocean isn't the only sink for CO_2 as primary productivity also lowers the ΔpCO_2, so then O_2 concentration and O_2 flux should be used to determine primary productivity in the mixed layer depth

Thus, if both CO_2 and O_2 budgets are measured using a simple model under constant pressure conditions at the surface, the total flux of CO_2 out of the water can be calculated as well as CO_2 flux out of the water only affected by primary production. I hypothesize then that I can quantify the proportion of the F_{CO2} caused by upwelling and primary productivity and F_{CO2} only caused by upwelling.

Methods

1. Shipboard Measurements

At each latitude, spanning from 5°N to 5°S (Table 1) , Sea-Bird SBE 911 plus a conductivity, temperature and depth (CTD) instrument attached to a 24-positions rosette with 10L Niskin bottles was deployed and surface seawater temperature, surface sea water salinity and dissolved oxygen (using a SBE43 DO sensor) were collected at specific depths. Wind speeds(in knots) from 2nd to 8th March, 2023 were obtained using a sonic wind sensor mounted on the RV Thompson which collected wind speeds every 10 seconds. An underway ΔpCO_2 system was attached to the research vessel and measurements at each latitude were acquired using this system.

2. Underway pCO_2 System for ΔpCO_2

The instrument was operated by NOAA PMEL Ocean Carbon program. The system directed the flow of seawater through the equilibrator chamber where seawater CO_2 equilibrated with the headspace gas in the chamber and then the CO_2 in the headspace gas was measured via a non-dispersive infrared analyzer, where the CO_2 mole fraction was obtained and then returned back to the equilibrator. The compound was calibrated using 4 CO_2 standard. Atmospheric gas was also pumped into the system to measure the CO_2 mole fraction. These mole fractions were reported dry as the CO_2 measurements were corrected with respect to the water vapor dilution and pressure effect internally by the analyzer itself (Pierrot et al, 2009).

3. Calibration of Oxygen

Oxygen samples were titrated using a standard method (Codispoti, 1988) and calibrated. Calibration also aided in removal of poor and inconsistent data. Samples for analysis of dissolved O_2 concentrations were collected from 1000-150m with ~200m intervals and 5-100m with 30m intervals between the depths. At the equator, the samples were taken from 5-4000m with 1000m, 200m and 25m intervals.

The dissolved O_2 was titrated using a Metrohm Dosimat 665 Titrator and used to calibrate the oxygen concetrations and oxygen percent saturations. 3 sample standards were made and 1 blank correction factor as well.

3.1 Titration of Samples

i) A clean stir bar was added to the sample and then 1ml H_2SO_4 was added and the solution was mixed well.

ii) The sample bottle was positioned on the stirrer with the buret tip submerged under the sample and the solution was tiratred by dispending thiosulfate into the sample. When the sample turned light yellow in color, 1ml of starch was added and the sample was titrated to the endpoint, when the solution turned sparkling clear.

iii) After the endpoint was recorded, the buret tip was rinsed with DI water to remove all residue.

3.2 Calibrating O_2 concentrations

In order to create a strong calibration, the titrated O_2 values were converted to µmol/kg and compared to the original O_2 sensor values. The O_2 concentrations obtained from the SBE43 sensor were then plotted against the titrated values and a calibration curve with a y=mx+b

equation was found. ~18% of the values were anomalies and considered bad or random data and omitted from the calibration curve.

4. CO_2 Flux calculation

CO_2 flux was quantified using the formula

$$F_{CO2} = k\ x\ Ksol\ x\ \Delta pCO_2 \quad \text{(Eq.2)}$$

Gas transfer velocity, k was calculated using the relationship

$$k = 0.251 * (V_{10})^2 * \left(\frac{Sc}{660}\right)^{-0.5} \quad \text{(Eq.3)}$$

where V is the wind speed and Sc is the Schmidt number of CO_2 or O_2 in seawater as a function of temperature (Wanninkhof, 2014). The Sc number was taken into account for the temperature variability and k was calculated according to those corresponding temperature of seawater for both the gases (Wanninkhof,1992). K_{sol} for CO_2 was calculated using the empirical relationship between temperature, salinity and solubility estimated by Weiss (1974). However, as $[O_2]_{atm}$ is considered constant, K_{sol} for O_2 was estimated with respect to the concentration of O_2 in equilibrium with the atmosphere.

5. *Carbon Budget Model Estimation*

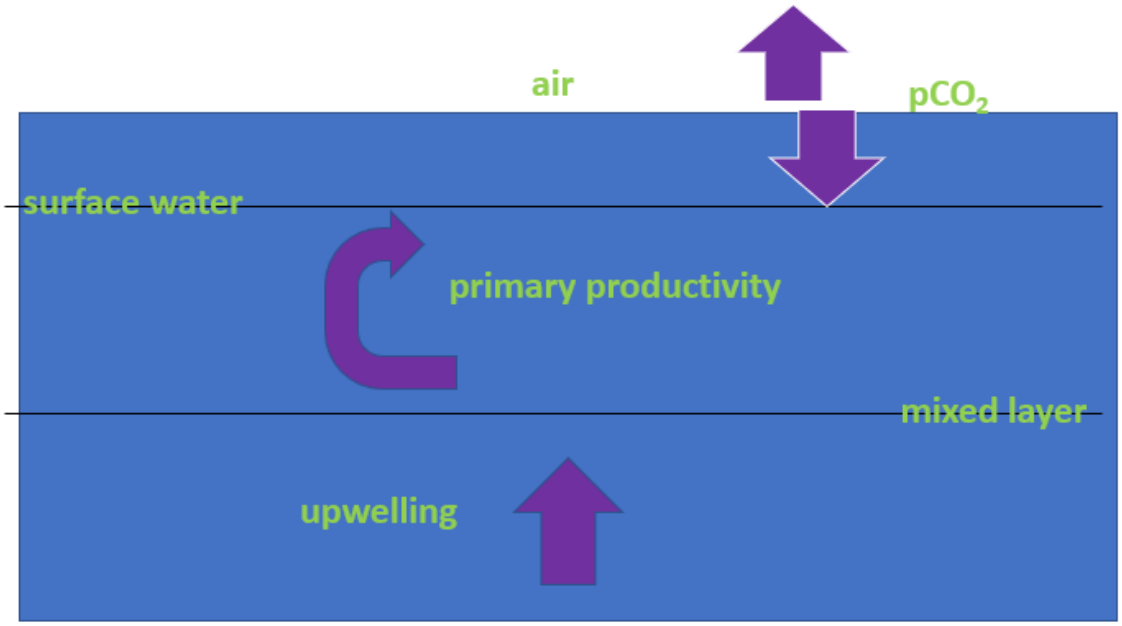

Figure 4: Rough schematic of 1-D Carbon Budget Model and contribution of each factor towards the Carbon Dioxide Balance in the Equatorial Pacific region.

A 1-D carbon budget model (Fig. 4) was estimated using a mixed layer model and the CO_2:O_2 Redfield ratio. The model was quantified using

$$\frac{dC}{dt} = F + J + u\Delta C \qquad \text{(Eq. 4)}$$

where F is the gas dependent flux (Eq.2) ,J is the primary productivity factor, uΔC (inferred as U also) is the upwelling flux is the upwelling factor and ΔC is the difference in concentrations from the deep and mixed layer (Emerson, 1987). For CO_2, a consistent value of deep-water concentrations was used averaged over the whole research transect, and the mixed layer depth concentration values were obtained from another researcher aboard the RV Thompson (DIC concentrations) (T.Dominguez, personal communication, 2023) while for O_2, the calibration curve equation was used to report the measured concentrations both in the mixed layer and below.

For simplification of the model, steady state was assumed ($\frac{dC}{dt} = 0$) ,vertical advection and horizontal and velocity along the mixed layer bottom boundary were assumed to be 0. To understand the proportion of the u and J and their contribution to the carbon budget, Eq.4 was modified in order to have 2 different simultaneous equations in the form of

$$u = \frac{-(F+J)}{C_d - C_{ml}} \quad \text{(Eq. 5).}$$

J is the biological consumption factor for CO_2 and the biological production factor for O_2 due to primary production (Emerson, 1987). Thus, an assumption based on Redfield ratios were used to correlate the biological factor, where $J_{O2} = -\frac{-106}{138} J_{CO2}$.

To understand how strong upwelling or primary productivity contributes in the fluctuation of the carbon budget at the equator, the values of F and ΔC were averaged from 2°N to 2°S.

Results

In order to calculate the magnitude of the gas fluxes, the initial approach was to determine the average daily gas exchange coefficient. The wind speed (U) m/s was then averaged out (using Coordinated Universal Time standards) to give the wind speed of each day. Sc value for CO_2 = 668 and Sc value for O_2 = 568 were used for k calculation (Wanninkhof, 1992 ; Wanninkhof, 2014). 2nd March was also included in the calculation to give an insight on the rate of change in wind speed and k values (Table 1). The wind speed significantly reduces going from 4th to 5th March and so do the k values of CO_2 and O_2. The research vessel was approaching the Eqautorial stations and transitioning into the Southern hemisphere, proceeding from 5th March and k is then observed to become relatively constant and have a lowered gradient change (Table 1).

Table 1: Daily Average wind speed (V) measured in m/s from March 2nd to 8th, 2023 and the corresponding Gas Transfer Velocities (k) measured in cm/hr for CO_2 and O_2 calculated at 180°based on the Sc temperature correlation, using UTC standard time. Positive latitudes correspond to the Northern Hemisphere and negative correspond to the Southern Hemisphere.

Date	Latitude	V (m/s)	kCO_2 (cm/hr)	kO_2 (cm/hr)
2-Mar-23	6°	11.474	32.849	35.623
3-Mar-23	5°	9.410	22.091	23.957
4-Mar-23	4°	10.437	27.176	29.472
	3°			
5-Mar-23	2°	6.275	9.823	10.653
	1.5°			
	1°			
	0.5°			
	0°			
6-Mar-23	0°	6.225	9.667	10.484
	-0.5°			
	-1°			
	-1.5°			
	-2°			
7-Mar-23	-2°	6.563	10.747	11.654
	-3°			
	-4°			
	-5°			

8-Mar-23	-5°	5.833	8.488	9.204

The change in k_{CO2} from 4th to 5th March is 17.35 cm/hr, which can be considered a steep gradient (Table 1). k_{CO2} = 27.176 cm/hr and k_{O2} = 29.472 cm/hr were the highest values recorded at V = 10.437 m/s on 4th March, 2023 corresponding to 3°N and 4°N (Table 1). The lowest V = 6.225 m/s and k_{CO2} = 9.667 cm/hr and k_{O2} = 10.484 recorded on 6th March, corresponding to stations at 0° to 2°S (Table 1).

Figure 5: Calibration curve of the O2 concentration (µmol/kg) collected using dissolved O_2 sensor 2 from March 3-8, 2023 along 5N to 5S at 180°

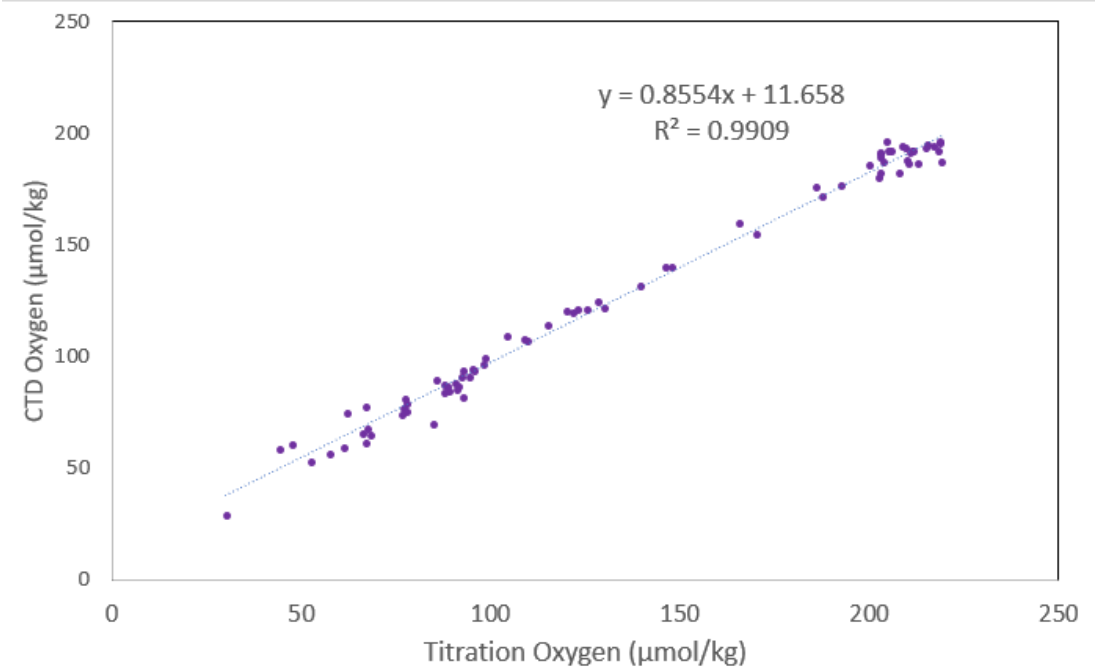

Dissolved O_2 values obtained from the SBE43 sensor were plotted against the titrated O_2 values to obtain a calibration curve (Fig 5). The equation of the line was used to convert the reported SBE43 dissolved O_2 concentrations and O_2 saturations to calibrated values.

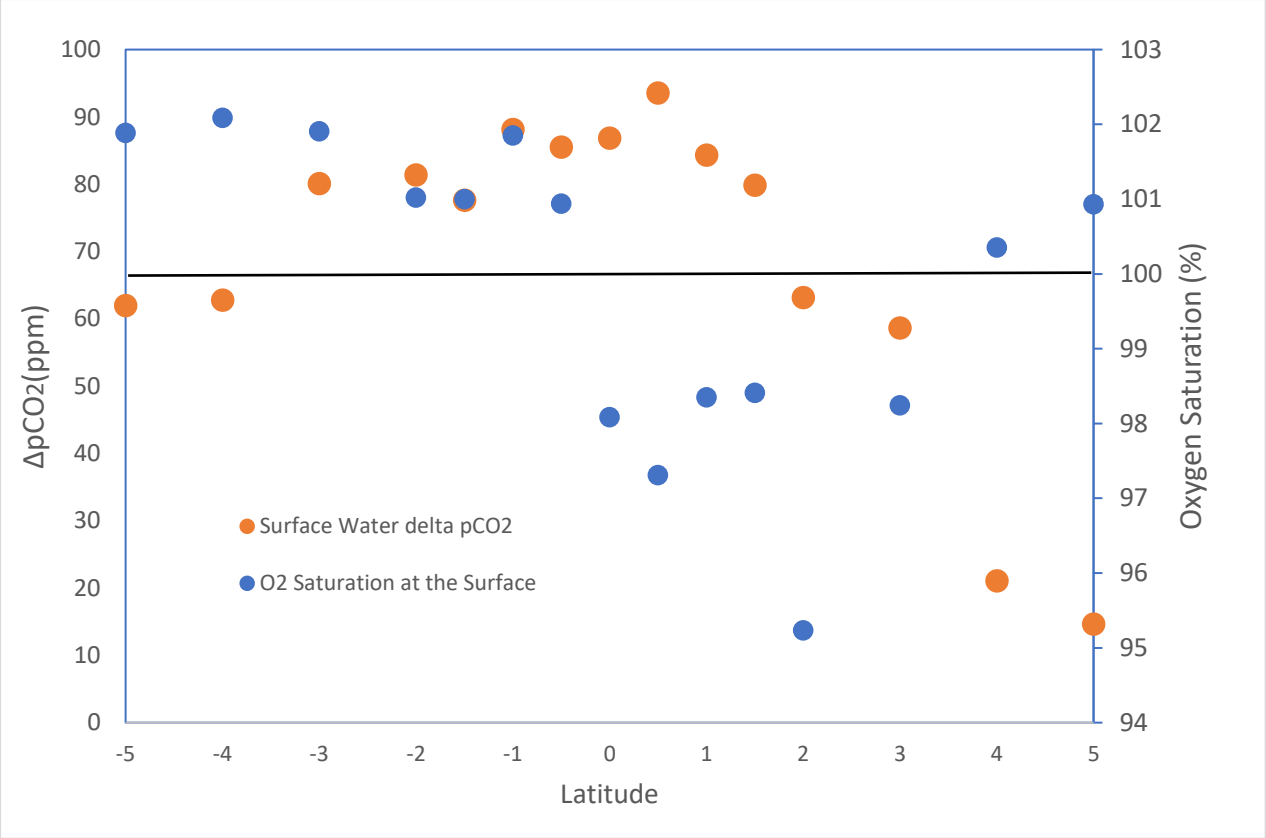

Figure 6: Surface Water CO_2 ΔpCO2 in ppm (Orange) and O_2 saturation Percentage (Blue) from 5N to 5S at 180° from 3rd-8th March, 2023. Horizontal line drawn at 100% O_2 saturation.

The average atmospheric pCO_2 during the survey was equal to 418.68ppm. ΔpCO_2 was plotted alongside the O_2 percentage saturation at the surface along the equatorial Pacific (Fig 6), where lowered oxygen saturation values are corresponding to a higher ΔpCO_2 closer to the equator(2°N - 2°S). The horizontal line differentiates the understaurated and saturated parts of equatorial Pacific, where anything below 100% O_2 saturation is undersaturated. The largest O_2 saturation gradient is at equator while the largest merdionial gradient in ΔpCO_2 is at 3°N. The lowest ΔpCO_2 = 14.68ppm, corresponds to a high Sat_{O2} = 100.92 at 5°N. Closer to the equator (1°N - 1°S), ΔpCO_2 is the highest with relatively lowered Sat_{O2}, except at 1°S where O_2 saturation = 101.85% and ΔpCO_2 = 88.14ppm. The highest ΔpCO_2 = 93.55pm at 0.5°N corresponding to a 97.31% of O_2 saturation. Even though, the lowest O_2 saturation =

95.23% was at 2°N with ΔpCO_2 = 63.18 ppm. As the transects moves from Northern equatorial Pacific to Southern Pacific, there's an increase in both ΔpCO_2 and Sat_{O2} at the surface (Fig 6).

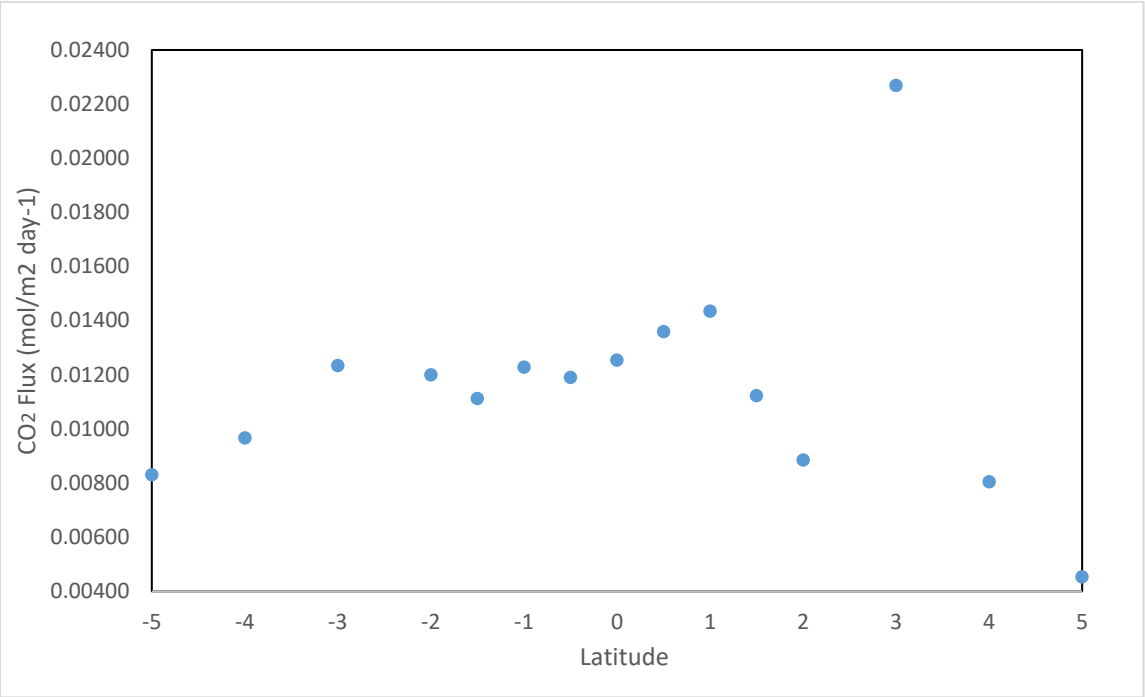

Figure 7: Flux of CO_2 (mol m^{-2} day^{-1}) of surface seawater from 5°N to 5°S at 180° from 3rd-8th March, 2023.

At 5°N, F_{CO2} = 0.00454 mol m^{-2} day^{-1} was recorded as the minimum calculated flux of CO_2 while at 3°N, F_{CO2} = 0.0227 mol m^{-2} day^{-1} was recorded as the highest flux of CO_2 (Fig 7). The daily flux in the Nothern hemisphere further away from the equator is observed to be relatively lower than in the Southern hemisphere

Since the wind speed decreases dramtically from 3°N to 2°N (Table 1) and to create a simple C budget, the results for F_{CO2} will be focused from 2°N - 2°S. The flux increases closer to the equator, with a peak at 1°N, F =0.0144 mol m^{-2} d^{-1} and then starts to gradually reduce transitioning from Northern transect into the Southern transect, except at 1°S, there's a slight peak with F = 0.0123 mol m^{-2} d^{-1} (Fig 7).

Table 2: ΔDIC and ΔO_2 measured in µmol/kg and their respective daily fluxes measured in mol m^{-2} day^{-1} from 2°N to 2°S between 5th-6th March, 2023 and the averaged values. Positive latitudes correspond to the Northern Hemisphere and negative correspond to the Southern Hemisphere.

Latitude	ΔDIC (µmol/kg)	ΔO_2 (µmol/kg)	F_{CO2} (mol/m^2 day^{-1})	F_{O2} (mol/m^2 day^{-1})
2°	2118.440	-96.686	0.0088	-0.000051
1.5°	2074.400	-77.569	0.0112	-0.000012
1°	2062.631	-99.295	0.0144	-0.000021
0.5°	2032.191	-77.553	0.0136	-0.000022
0°	2050.232	-74.479	0.0125	-0.000015
-0.5°	2059.534	-101.438	0.0123	0.000010
-1°	2052.608	-73.430	0.0111	0.000013
-1.5°	2075.133	-105.291	0.0120	0.000011
-2°	2070.397	-84.811	0.0123	0.000008
Average	2066.174	-57.940	0.0120	-0.000009

The flux of CO_2 from 2°N to 2°S was then averaged = 0.0120 mol m^{-2} day^{-1} (Table 2). Average F_{O2} = -0.000009 mol m^{-2} day^{-1} (Table 2). F_{O2} from 2°N-0° is observed to be negative, which is a flux into the system while F_{O2} starting from 0.5°S is calculated to be positive, a flux out of the system. Note that $[CO_2]_{deep}$ = 2285 umol/kg and ΔDIC were calculated based on this equilibriated $[CO_2]_{deep}$ value. ΔDIC and ΔO_2 were multiplied by density (kg/m^3) where the

mixed layer began, to convert into units of volume and then ultimately multiplied by k and K_{sol} to obtain the gas fluxes in mol m^{-2} day^{-1}.

Solving the system of equations for u and J using a variation of Eq.4 (Emerson, 1987) to account for the direction of the flux.

i) CO_2

$$0 = -F[CO_2] + u(\Delta CO_2) - J[CO_2]$$

ii) O_2

$$0 = -F[O_2] + u(\Delta O_2) - \frac{106}{138}J[CO_2]$$

$$0.00206617u - J = 0.01204$$

$$0.00005794u + 0.768J = 0.000009$$

$u = 5.627$

$J = -0.000413$ mol m^{-2} day^{-1}

$U = 0.0116$ mol m^{-2} day^{-1}

The overall upwelling term, U is equal to 0.011 mol m^{-2} day^{-1}, that is ~96.3% of the CO_2 flux while primary productivity, J contributes ~3.3% towards the flux (Fig.8). The average ΔpCO_2 in this region was equal to 82.3 ppm.

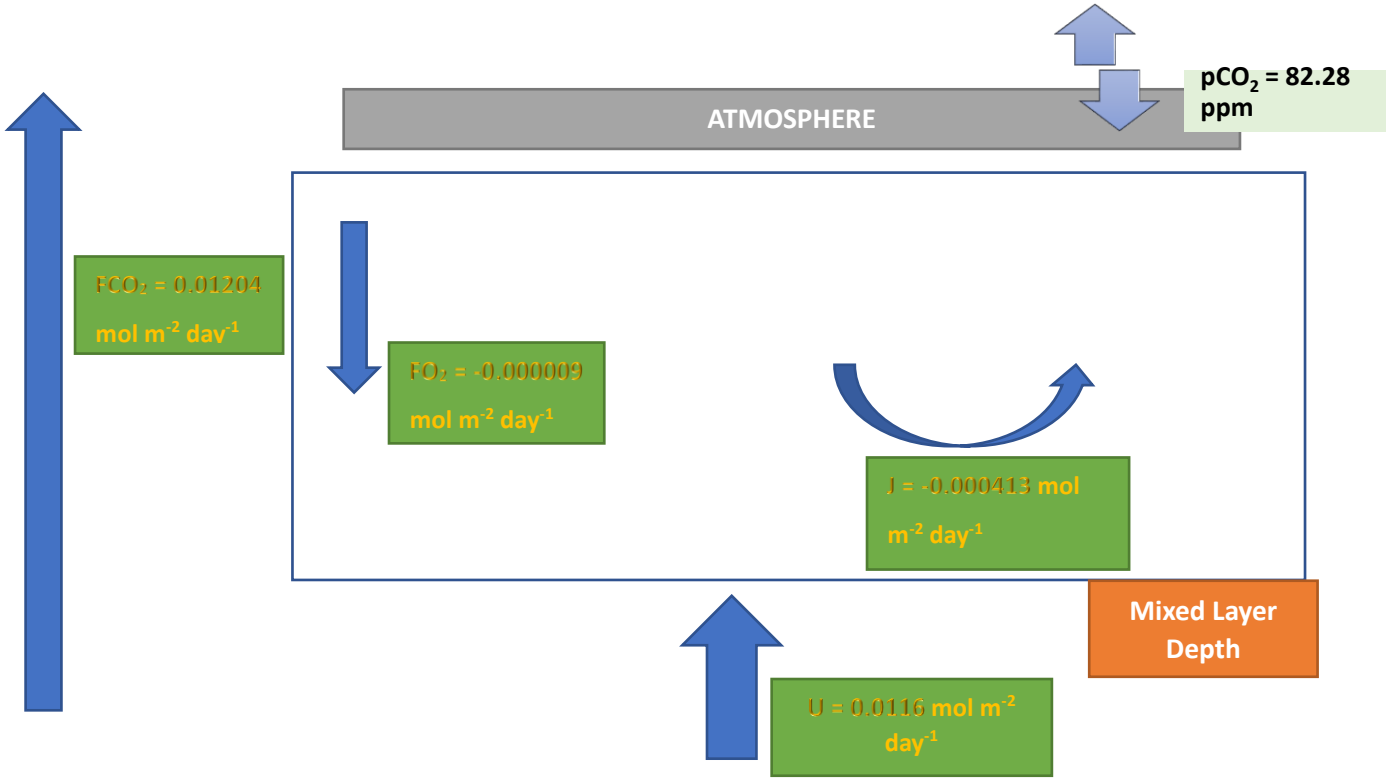

Figure 8: Schematic of 1-D Carbon Budget Model, interaction between atmosphere and the ocean, O_2 and CO_2 fluxes, and contribution of primary productivity (J) and upwelling (U) towards the Carbon Dioxide Balance in the Equatorial Pacific from 2°N to 2°S. All variables are in units of mol m^{-2} day^{-1} except pCO_2 (ppm).

To understand if the ENSO cycle (end of the La Niña) could potentially affect the CO_2 and O_2 fluxes, they were converted into an annual flux, where F_{CO2} = 4.395 mol m^{-2} yr^{-1} and

F_{O2} = -0.003285 mol m^{-2} yr-1, respectively in the Equatorial Pacific.

Discussion

The ocean is one of the biggest sinks of CO_2 and plays an integral role in maintaining the CO_2 inteeraction between the atmosphere and ocean, sequestring more than producing (Friedlingstein et al, 2022 ; Hauck et al, 2020). However, the equatorial Pacific is a unique region where CO_2 leaves the system, or rather acts as a source for CO_2 and outgasses into

the atmosphere (Pitmann et al, 2022). The CO_2 concentration is affected by many variables such as SST, wind speed, ENSO phases, upwelling and the primary productivity, where primary producitvity acts as a sink.

1.1 Physical drivers of F_{CO2}

The average daily wind velocities seem to be decreasing as it gets closer to the equator (Table 1). Even though the winds are decreasing, the CO_2 flux is positive (Fig 7) and out of the system. According to Eq.2, the flux is dependent on k, the gas transfer velocity so the extremely high value of F_{CO2} at 3°N can be correlated more to high wind speeds and high k value (Fig 7) than ΔpCO_2 value of 58.63 ppm. When looking at previous studies conducted by NOAA Pacific Marine Environmental Labroratory (PMEL) in the equatorial Pacific, the yearly flux during a non-El Niño is positive and out of the system and is within the range of 0-7 mol m^{-2} yr^{-1-}. The F_{CPO2} = 4.4 mol m^{-2} yr^{-1} calculated during this research falls within that range, implying that this relatively cooler region is contributing to new CO_2 production and a stronger flux out of the oceanic system but is not entriely dependent on a neutral or La Niña phase as wind speeds significantly reduced starting from 2°N, indicating that other factors may be playing a bigger role in determining the positive outgassing of CO_2.

1.2 ΔpCO_2 and O_2 saturation

Dissolved O_2 values were calibrated in order to reduce errors and standardize the concentrations without too much variability. Due to the upwelled waters being rich in DIC concentrations, it can explain how O_2 is undersaturated in this equatorial region (Fig.6). MLD being source of CO_2 due to nutrient-rich waters being transported up the water column would lead to a higher rate of primary productivity and ultimately higher O_2 production (Sutton et al,2017) but that did not seem the case at this specific time period. Additionally,

$J \approx -0.0004$ mol m^{-2} day^{-1} implies that rather than primary productivity being a sink for carbon, it essentially is negligible in the carbon budget since it is contributing <4% to the CO_2 flux. The negative magnitude also implies that there may have been a higher rate of respiration, where oxygen was being consumed faster than being produced (Emerson and Yang, 2022 ; Honjo et al, 2014). This lowered saturation of O_2 could also explain the negative F_{O2} averaged over 2°N to 2°S (Table 2). In contrast, the ΔpCO_2 values are increasing moving from 2N, peaking at 0.5°N, staying above the 100% saturation line (Fig 6) and then gradually reducing when leaving the main equatorial basin. Additionally, F_{CO2} is also dependent on the positive ΔpCO_2 (Eq 1), which implies that the $[CO_2]$ in seawater was much more than the atmosphere (Fig 5), thus providing evidence that the equatorial Pacific is a source of CO_2 and that rate of primary production is not able to overcome the rate at which CO_2 is being upwelled. Another thing to note is that from 2°N to 0°, O_2 sat is under 100%, which could explain the negative F_{O2} in the Northern Hemisphere from 2°N to 0° (Fig 6, Table 2) as there is just not enough O_2 being produced.

The relatively higher ΔpCO_2 values can also be used to understand the low O_2 saturation percentage, where higher rates of respiration are occuring and primary production is still taking place but not dominating the biological pump's effect on carbon storage.

1.3 Upwelling and F_{CO2}

Previous studies by Sutton and Pittman provide evidence that upwelled DIC can be distributed in various ways throughout the ocean system, either by outgassing, advecting horziontally or exported to the deep ocean. For this study conducted in the equatorial Pacific, upwelling of cold nutrient-rich waters leads to a CO_2 flux leaving the system and ultimately being vertically moved out of the system. Upwelling accounts for more than 95%

of the flux exiting the system (Fig.8) and can be assumed to be the main driver of the CO_2 and increased saturation in surface and mixed layer waters. Averaged yearly

F_{CO2} = 4.4 mol m^{-2} yr^{-1} (2°N to 2°S) should be considered significant enough to perturb the C-cycle as the equatorial Pacific is huge and changes in CO_2 flux on an annual basis is mainly caused by rate of upwelling(https://www.pmel.noaa.gov/co2/elNiño.html). It should be acknowledged that there were time constraints during the course of the research and various steady-state assumptions, espeically related to horizontal advection of water and were included in the calculations in order to create a 1-D C budget model.

The highest recorded flux of CO_2 was at 3°N (Fig 6) but when only considering the transect 2°N to 2°S, the highest flux out of the system was at 1°N, which is interesting as the highest ΔpCO_2 was at 0.5°N (Fig 5) and both the stations at these latitudes had the same k value (Table 1). The only difference was the ΔCO_2 values (Table 2). ΔCO_2 for 1N = 2062 umol/kg while 0.5°N = 2032 umol/kg. This implies that at 1°N, the surface waters were slightly more saturated with CO_2 than at 0.5°N.

Upwelling played a substantial role in determining the carbon budget model in the equatorial Pacific and even though primary production was not as significant in budgeting the carbon concentrations, my hypothesis was able to be proved and that was the quantification of ΔpCO_2 in order to calculate the outgassing of CO_2 and understand the significance of upwelling and primary productivity's contirbution to the carbon buget balance in the equatorial Pacific. If it was also possible, I would have liked to utilize advection of air-sea flux to determine analytically how much could heat contribute to the carbon balance (Wong et al, 2022). This 1-D carbon model does not have different sources of

atmospheric carbon entering the ocean and is rather equilibriated to one value but if it did, it could extend the scope of the budget model even more.

If time and resources permitted, chlorophyll and nutrients such as iron or nitrogen could also have been analyzed to understand the anomalous nature of primary productivity and how this phenomenon was not able to act as a strong sink for CO_2 or even a strong source for O_2. Additionally, using Emerson's mixed layer formula variables such as MLD height and the vertical transport across the bottom boundary layer could potentially provide even more accurate values for upwelling and primary producion fluxes which ultimately influence the C balance of the ocean, specifically the equatorial Pacific.

Conclusion

A carbon budget model is utilized to understand the effects of different factors, be it biological or physical on the carbon cycle and how proportionately they contribute to the C concentrations, either in the ocean or out of the ocean. The ocean is generally a sink of CO_2, uptaking it to carry out primary production and stabilize the C-cycle. However, a unique region such as the equatorial Pacific acts as source of CO_2 instead due to the high rates of upwelling, which brings up nutrient rich waters from the deep ocean to the mixed and surface layers. This phenomenon then tends to increase the concentrations, which leads to a flux of CO_2 out of the system, or outgassing. The equtorial Pacific is a source of CO_2 and sink of O_2. Even though physical factors such as k and K_{sol}, which is dependent on salinity are considered, it is evident that upwelling seems to play the biggest role in influencing the rate of change in carbon concentration ~96% of the flux. Additonally, wind speed and k also dropped sharply 27 cm/hr at 3°N to 9.8 cm/hr at 2°N and then stayed relatively even ~9cm/hr closer to the equator. This implied that wind could not have perturbed the F_{CO2}

immensely and cause the surface waters to be extremely saturated. But rather, it was the upwelling flux, that affected the CO_2 outgassing event from the equatorial Pacific. It is important to acknowledge that during periods of high upwelling, where DIC rich waters are surfacing, the water is expected to undersaturated in O_2 which led to F_{O2} -0.000009 mol m^{-2} day^{-1}. However, it is surprising that even though the rate of nutrient and DIC influx into the mixed layer is high, the biological factor, J= -0.0004 mol m^{-2} day^{-1} has a negative flux, indicating that primary production may not be occuring at a rate fast enough to counter upwelled waters. But on an annual scale, the F_{CO2} = 4.395 mol m^{-2} yr^{-1} is well within the expected range during a non-El Niño event. Difference in ENSO phases and how a warm phase vs a cold phase can really affect CO_2 saturation state and upwelling rates. Using the model which considers ΔpCO_2, the daily CO_2 flux and primary production through an O_2 proxy, can be insightful towards future models of open oceans and their contribution to the carbon budget and aid in quantifying natural vs anthropogenic sources of CO_2 and their proportion of contribution towards climate change, increase in global temperatures and even ocean acdification due to increased uptake of inorganic carbon.

In a broader sense, the equatorial Pacific is open ocean source of carbon but as anthroprogenic emissions for CO_2 continuously rise, it is possible to that due to the inability to overturn inorganic carbon to organic matter fast enough, many other parts of the ocean may become a source as well rather than a sink. Therefore, to understand how the atmospheric concentration of CO_2 is changing with respect to the ocean in upwelling regions, further studies could be conducted for prolonged periods of time to truly determine if the equtorial Pacific will remain a strong source of outgassing CO_2 system, even when compared to other areas of upwelling or could it possibly also act as a sink, depending on the strength of the biological and solubility pumps.

Acknowledgements

I would like to express my gratitude towards the captain, crew and science team of the RV TG Thompson for aiding in my research and helping me to obtain my data. I would also like to express my thanks to my classmates and peers without whom I would not have been able to collect and process data as quick as I did. I would also like to thank the professors in charge of the senior thesis, especially Mark Warner, Kathy Newell and Rick Keil for supporting me in my scientific endeavours and guiding me on the correct path for my project, data analysis and thesis.

References

Emerson, S. (1987), Seasonal oxygen cycles and biological new production in surface waters of the Subarctic Pacific Ocean, *Journal of Geophysical Research*, *92*(C6), 6535, doi:10.1029/jc092ic06p06535.

Emerson, S., and B. Yang (2022), The Ocean's biological pump: In situ oxygen measurements in the subtropical oceans, *Geophysical Research Letters*, *49*(21), doi:10.1029/2022gl099834.

Friederich, G. E., J. Ledesma, O. Ulloa, and F. P. Chavez (2008), Air–sea carbon dioxide fluxes in the coastal southeastern Tropical Pacific, *Progress in Oceanography*, *79*(2–4), 156–166, doi:10.1016/j.pocean.2008.10.001.

Friedlingstein, P. et al. (2022), Global Carbon Budget 2021, *Earth System Science Data*, *14*(4), 1917–2005, doi:10.5194/essd-14-1917-2022.

Gloege, L., M. Yan, T. Zheng, and G. A. McKinley (2022), Improved quantification of ocean carbon uptake by using machine learning to merge Global Models and PCO2 data, *Journal of Advances in Modeling Earth Systems*, *14*(2), doi:10.1029/2021ms002620.

Gruber, N. et al. (2009), Oceanic sources, sinks, and transport of atmospheric CO2, *Global Biogeochemical Cycles*, *23*(1), doi:10.1029/2008gb003349.

Hauck, J. et al. (2020), Consistency and challenges in the Ocean Carbon Sink estimate for the Global Carbon Budget, *Frontiers in Marine Science*, *7*, doi:10.3389/fmars.2020.571720.

Heinze, C., S. Meyer, N. Goris, L. Anderson, R. Steinfeldt, N. Chang, C. Le Quéré, and D. C. Bakker (2015), The Ocean Carbon Sink – Impacts, vulnerabilities and challenges, *Earth System Dynamics*, *6*(1), 327–358, doi:10.5194/esd-6-327-2015.

Honjo, S. et al. (2014), Understanding the role of the biological pump in the global carbon cycle: An imperative for ocean science, *Oceanography*, *27*(3), 10–16, doi:10.5670/oceanog.2014.78.

Johnson, K. S. (2010), Simultaneous measurements of nitrate, oxygen, and carbon dioxide on Oceanographic Moorings: Observing the Redfield Ratio in real time, *Limnology and Oceanography*, *55*(2), 615–627, doi:10.4319/lo.2010.55.2.0615.

Murray, C. N., and J. P. Riley (1969), The solubility of gases in distilled water and sea water—II. oxygen, *Deep Sea Research and Oceanographic Abstracts*, *16*(3), 311–320, doi:10.1016/0011-7471(69)90021-7.

Pierrot, D., C. Neill, K. Sullivan, R. Castle, R. Wanninkhof, H. Lüger, T. Johannessen, A. Olsen, R. A. Feely, and C. E. Cosca (2009), Recommendations for autonomous underway PCO2 measuring systems and data-reduction routines, *Deep Sea Research Part II: Topical Studies in Oceanography*, *56*(8–10), 512–522, doi:10.1016/j.dsr2.2008.12.005.

Pittman, N. A., P. G. Strutton, R. Johnson, R. J. Matear, and A. J. Sutton (2022), Relationships between air-sea co 2 flux and new production in the Equatorial Pacific, *Global Biogeochemical Cycles*, *36*(4), doi:10.1029/2021gb007121.

Redfield, Alfred Clarence. "On the proportions of organic derivatives in sea water and their relation to thecomposition of plankton." James Johnstone memorial volume (1934): 176-192

(1) (PDF) ON THE PROPORTIONS OF ORGANIC DERIVATIVES IN SEA WATER AND THEIR RELATION TO THE COMPOSITION OF PLANKTON This is the text from Alfred Charles Redfield paper. Available from: https://www.researchgate.net/publication/344709447_ON_THE_PROPORTIONS_OF_ORGANIC_DERIVATIVES_IN_SEA_WATER_AND_THEIR_RELATION_TO_THE_COMPOSITION_OF_PLANKTON_This_is_the_text_from_Alfred_Charles_Redfield_paper [accessed May 10 2023].

Sutton, A. J., R. Wanninkhof, C. L. Sabine, R. A. Feely, M. F. Cronin, and R. A. Weller (2017), Variability and trends in surface seawater *p*co2 and co2 flux in the Pacific Ocean, *Geophysical Research Letters*, *44*(11), 5627–5636, doi:10.1002/2017gl073814.

Takahashi, T. et al. (2009), Climatological mean and decadal change in Surface Ocean PCO2, and net sea–air CO2 flux over the Global Oceans, *Deep Sea Research Part II: Topical Studies in Oceanography*, *56*(8–10), 554–577, doi:10.1016/j.dsr2.2008.12.009.

Tian, F., R.-H. Zhang, and X. Wang (2019), Factors affecting interdecadal variability of air–sea CO2 fluxes in the tropical Pacific, revealed by an ocean physical–biogeochemical model, *Climate Dynamics*, *53*(7–8), 3985–4004, doi:10.1007/s00382-019-04766-5.

Vaittinada Ayar, P., J. Tjiputra, L. Bopp, J. R. Christian, T. Ilyina, J. P. Krasting, R. Séférian, H. Tsujino, M. Watanabe, and A. Yool (2022), *Contrasting projection of the enso-driven co₂ Flux Variability in the equatorial Pacific under high warming scenario*, doi:10.5194/esd-2022-12.

Volk, T., and M. I. Hoffert (1985), Ocean Carbon Pumps: Analysis of relative strengths and efficiencies in ocean-driven atmospheric CO2 changes, *The Carbon Cycle and Atmospheric CO2: Natural Variations Archean to Present*, 99–110, doi:10.1029/gm032p0099.

Wanninkhof, R. (1992), Relationship between wind speed and gas exchange over the Ocean, Journal of Geophysical Research, 97(C5), 7373, doi:10.1029/92jc00188.

Wanninkhof, R. (2014), Relationship between wind speed and gas exchange over the ocean revisited, *Limnology and Oceanography: Methods*, *12*(6), 351–362, doi:10.4319/lom.2014.12.351.

Weiss, R. F. (1974), Carbon dioxide in water and seawater: The solubility of a non-ideal gas, Marine Chemistry, 2(3), 203–215, doi:10.1016/0304-4203(74)90015-2.

Wong, S. C., G. A. McKinley, and R. Seager (2022), Equatorial Pacific PCO 2 interannual variability in CMIP6 models, *Journal of Geophysical Research: Biogeosciences*, *127*(12), doi:10.1029/2022jg007243.